RELATIONSHIP BETWEEN M8+ EARTHQUAKE OCCURRENCES AND THE SOLAR POLAR MAGNETIC FIELDS

Ben DAVIDSON[1,2,*], Kongpop U-YEN and Christopher HOLLOMAN[3]

*Corresponding Author: Space Weather News LLC - ben@observatoryproject.com
[1] The Mobile Observatory Project
[2] Space Weather News LLC
[3] Ohio State University Statistical Consulting Service

Abstract: The Sun's polar magnetic fields modulate many aspects of space weather and the local space environment. The magnetism of the solar polar fields (SPF), as measured by the Wilcox Solar Observatory (WSO), have been studied and compared with the large magnitude earthquake record from the United States Geological Survey. The time period covers the 38 years (+13,600 days) that the WSO has collected the SPF data, up to January 2014. This study reveals a dependence of M8.0+ seismicity on the oscillations of the SPF; the extremes in magnetism of the polar fields, and their polarity reversals, may be modulating the largest earthquakes on the planet.

Keywords: space weather, solar polar magnetic fields, piezoelectricity, global electric circuit, magnetic fields, M8+, largest earthquakes

INTRODUCTION

The solar polar fields are a significant electromagnetic factor in space weather and the ambient environment of the inner heliosphere. To think of space as an empty vacuum does not adequately represent the scope of interaction between the Earth and Sun. The Earth orbits in an electric field of charged solar wind particles, bathed in varying levels of x-ray and extreme ultraviolet radiation, and connected directly to the Sun through the interplanetary magnetic fields. Scientists have been trying to correlate solar activity with seismicity for decades, but focus has centered on sunspots, solar flares and geomagnetic indices. Rather than studying the space weather mitigated by earth's magnetosphere we studied the interplanetary magnetic fields of the Sun's poles. The magnetosphere is known to open up to these magnetic portals to the Sun (Phillips, 2008) every few minutes, and have effects on a much larger scale than single space weather events. The solar polar field fluctuations appear to modulate the occurrences of the Earth's largest seismic events.

THE SOLAR POLAR FIELDS (SPF)

The Sun has north and south magnetic poles that reverse every solar sunspot cycle, or every ~11 years. The SPF measured at Earth also oscillate between significantly greater and lesser magnetism over shorter periods of ~1 year. The large ~1-year oscillations in magnetism (**Figure 1**) can be explained by changes in the heliospheric latitude of Earth's orbit (Babcock 1955; Svalgaard 1978). The polar fields on the Sun are persistently parallel to the polar fields of Earth (Babcock, 1959), which means that Earth orbits the at approximately the equator of the Sun, but not exactly; earth's position in the heliosphere determines which solar pole is closer to earth, and influences which of the SPF is more influential over the local solar wind environment. The SPF have been measured consistently since May 1976, when the Wilcox Solar Observatory (Stanford University) began collecting a running record of 10-day averages. These data can be visually represented as shown **Figure 1**.
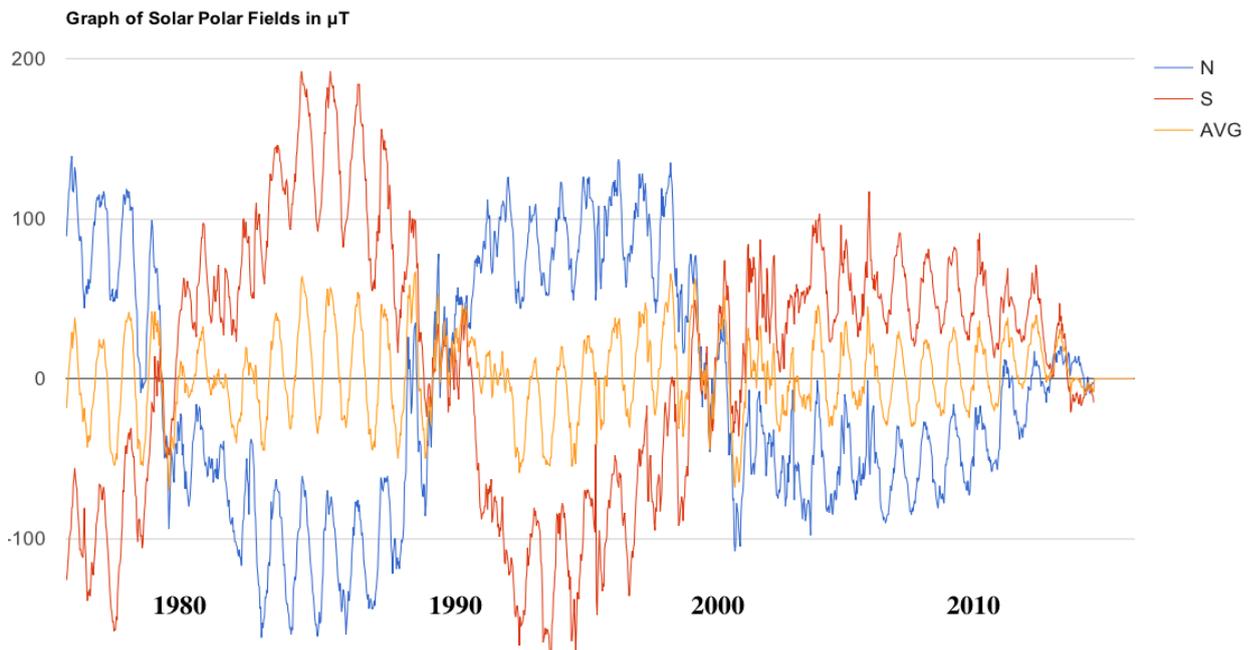
Fig. 1. Graph of Solar Polar Fields in µT. Solar Polarity Data adapted from the website of the Wilcox Solar Observatory. The Blue line is the North SPF, while the Red line is the South SPF. The Yellow line represents the Average Polar Magnetism of the two fields. Here we see a sinusoid on a large scale (~11 year solar cycles) and a small scale (~1 year). The Y-axis and baseline around which the solar poles are plotted is 0 µT. Above the baseline is positive polar magnetism, and below the baseline is negative polar magnetism - the further the line goes up or down, away from the central baseline, the stronger the magnetism.

During SPF reversals, each pole may reverse numerous times in a period that lasts more than a year. The SPF are weakest during the reversal, which occurs at sunspot maximum, and they are strongest during sunspot minimum; the cycles are inverse but in sync. Sunspot maximum occurs during the minimum magnetism of the polar fields, "Polar Minimum," while sunspot minimum occurs during "Polar Maximum."

Polar Minimum begins after both of the Sun's poles have reversed their polarity once during the sunspot maximum (rarely do north and south begin reversing together) and ends after the final reversal of sunspot maximum. After Polar Minimum, the SPF begin to steadily increase in magnetism in the opposite direction (+/-) from their polarity during the previous cycle. After approximately 18 months of "Polar Recovery" (~1.5 ~1-yr oscillations) the SPF have strengthened enough to be characterized as Polar Maximum, which lasts until the next Minimum begins.

In **Figures 2 and 3** we see a qualitative view of the SPF cycle, and an example of Polar Minimum, Polar Recovery and Polar Maximum, respectively.
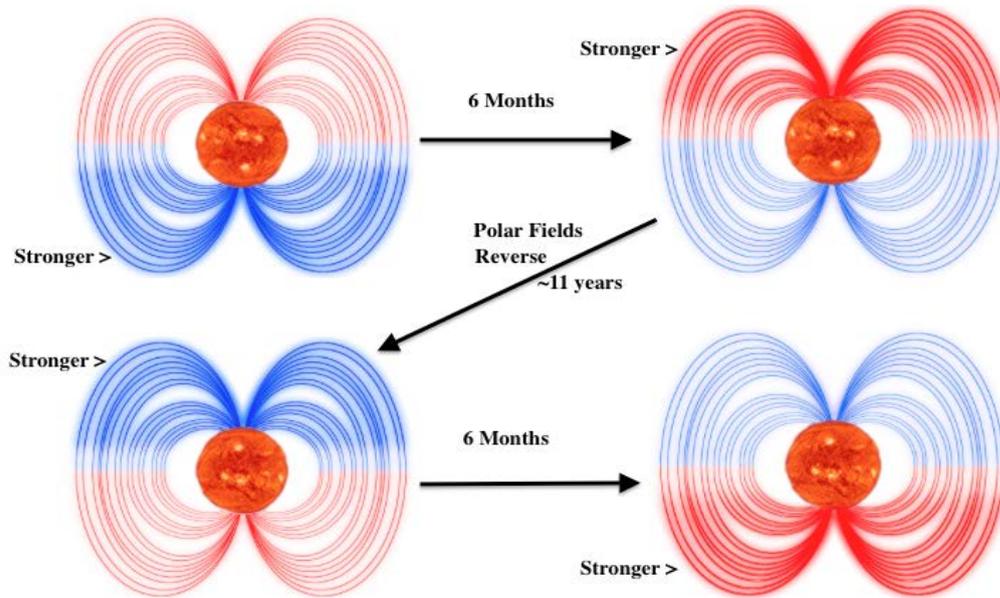
Fig. 2. Visual Representation of the ~1-year/~11-year Oscillations of the SPF. The top two images represent the shifting between N and S polar field strength, usually ~6 months apart. Top left we see thicker, bolder blue lines, representing stronger force to the southern pole. Top right we see thicker, bolder red lines, representing stronger force to the northern pole. The bottom two images are after a pole reversal has taken place, which occurs every ~11 years, and represent the same pattern of magnetic force alternating between N and S.
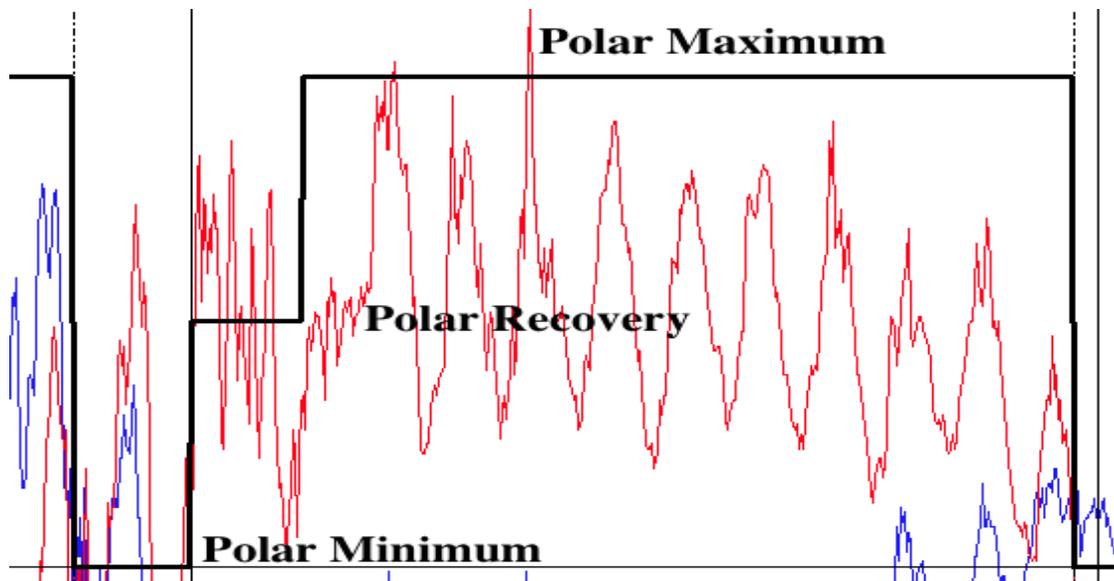

Fig. 3. Example of the Separation of Phases in the Solar Polar Fields Cycle Polar Minimum, Recovery, and Maximum are shown here using a portion of the SPF data. The minimum shown here is the reversal that occurred from 1999-2001, followed by ~18 months of recovery, and then the maximum period. The full SPF data, broken down into the SPF phases can be seen in Appendix B. This pattern holds true for both poles, during both positive and negative phases of their cycles.

SIGNIFICANT WINDOWS OF SPF FOR TRIGGERING TECTONIC STRESS

"Significant Windows" cover periods of time when we hypothesized that the SPF could trigger seismic activity: (1) the extremes in SPF magnetism (either positive or negative), which are visualized as the peaks and troughs in **Figures 1 and 3**, and (2) the changes in polarity of the SPF, both individually and as a combined average, which are visualized as the lines crossing the central baseline in **Figure 1**, and the color reversal in **Figure 2**. The dates of extremes in magnetism and polarity reversals are surrounded by a Significant Window of days during which an M8+ Earthquake would be considered 'covered' within the window.

For the extremes in magnetism, the strength of the peaks alters the length of the Significant Window, where the strongest peaks have slightly longer windows than other peaks. Some extreme periods in SPF magnetism have multiple peaks/troughs, during which times the Significant Windows were split and shared by the peaks in force. The time periods around the peaks in solar polar magnetism should be the times when the polar fields affect Earth the most, and therefore are logical factors in Significant Windows. We also looked at two kinds of SPF reversals for the Significant Windows: 1) the reversal of each individual hemispheric polar fields, a "Pole Reversal," and 2) the reversal of the average polar magnetism of the Sun, an "Average Reversal," derived by adding the northern fields magnetism to the southern fields magnetism, and visualized as the yellow curve in **Figure 1**. For each individual pole, the first and final reversal of each Polar Minimum is significant, and if there are more than two reversals in such a period, the magnetism must increase beyond a threshold of minimum intensity in order for the subsequent Pole Reversal to be considered significant. For the Average Reversals of the Sun, there must be adequate time between reversals for them to be considered significant; the hypothesis is that multiple short-term reversals would not allow the Earth dynamo to build-up the stress requisite for a M8+ earthquake. The two types of polar reversals are significant SPF features because they are the moment when the force of the SPF changes direction; a push becomes a pull, or a pull becomes a push.

The Delay Factor
The above conditions determine whether each time point falls into a Significant Window, but the occurrence of earthquakes can reduce the likelihood of a subsequent earthquake due to the release of pressure and stress in the crust. To allow for accumulation of stress, we delay Significant Windows that occur soon after the earthquake. Each time a M8+ or series of slightly smaller earthquakes (Four M7.5+ earthquakes in a 100 day window) occurs, Significant Windows occurring in the next 100 days are delayed. For Significant Windows starting less than 30 days after the occurrence of one of these earthquake events, the window is pushed back by the lesser of either 20 days or up to the date of the factor creating the Significant Window. For Significant Windows starting between 31 and 100 days after the occurrence of one of these earthquake events, the window is pushed back by 10 days.

ANALYZING THE SIGNIFICANT WINDOWS AND EARTHQUAKE EVENTS
The factors for creating Significant Windows are simple, but communicating them mathematically is more complex. The SPF data and the earthquake history were compared using the simple factors for Significant Windows and translated into a mathematical algorithm (**Appendix A**). The data analysis was performed using R code for statistical computing (Holloman, 2014). The analysis probed the earthquake data for dependence on SPF measurement. Using these rules, we surveyed the +13,600 days covered from June of 1976 through mid-January 2014 to create the Significant Windows of solar polarity, which, based on the hypothesis embodied in the identification of the Significant Windows, could be proliferative to earthquake activity. The result yielded 41.6% of the days as 'significant.' For statistical testing, our null hypothesis is that the timing of occurrence of the largest earthquakes is independent of the Significant Windows of solar polarity. Under this hypothesis, one would expect approximately 41.6% of the earthquakes over the time period to fall within the Significant Windows. There were thirty-three M8+ earthquakes that were recorded on Earth between mid-1976 and mid-January 2014, according to the records from United States Geological Survey. Assuming the independence of Significant Windows and earthquake occurrence, the probability of each of the 33 M8+ earthquakes of falling within Significant Windows is 41.6%. Twenty-six of the thirty-three M8+ earthquakes (78.8%) fall within the Significant Windows. Given the probability at the outset, and assuming there is no relationship between SPF and M8+ earthquakes, the probability that 26 or more out of 33 such events fall within Significant Windows is;

$$\text{Probability} = \sum_{i=26}^{33} \binom{33}{i} X^i (1-X)^{33-i},$$

where X represents the probability that an earthquake will fall within a Significant Window (41.6%). Probability = 0.000015.

Although the p-value is small, it is likely heavily biased since it is calculated against the SPF dataset that was used to refine the theoretical development of the algorithm. Despite this bias, we believe it provides

substantial evidence against an assumption that solar magnetism is unrelated to occurrence of M8+ earthquakes. The SPF data set was used to formulate the descriptions of the Significant Windows but was done so independent of the seismic event catalogue. The calculated p-value is 0.000015 (about 1 in 90,000), providing very strong evidence against the null hypothesis. Our statistical analysis demonstrated that numerical algorithms can be used to extract important features from 10-day averages of SPF indices. These extracted features can then be used to identify windows of time during which large earthquakes are more likely to occur or not occur. The features that are selected by the algorithms are relatively straightforward, consisting of the aforementioned peaks and troughs in magnetism, and times of polarity reversal. Although the results of this study are promising, it should be noted that the analysis was performed retrospectively, meaning that the model currently lacks a predictive element, and must assessed by examining how well it predicts large earthquakes in the future.

DISCUSSION
This analysis suggests that M8+ seismicity is dependent on the variations in the SPF. Now we will discuss the most likely ways to improve our algorithm, a model for a explaining the SPF trigger mechanism, how the SPF might be interacting with the Earth, why considering the relationship between electromagnetism and earthquakes may help us better-understand these M8+ disasters, what to look for in the coming SPF cycles, and the scope of the relationship implied by this study.

Improving this model in the future
This current model affords confidence in the relationship between SPF and M8+ earthquakes, but it needs to be refined. In reviewing the analysis it is clear where we need to refine this model in the future; we need to revise Significant Windows around extremes in magnetism, and reconsider the entire period of Polar Recovery.

The rules for significant windows around extremes in magnetism should be revisited
Among the seven M8 earthquakes that were not covered by the Significant Windows, a few were so close to being 'covered' that it suggests that we may not understand the breadth of the Significant Windows. Among those situations, none are more glaring than the only day with two M8 earthquakes on record, April 11, 2012, illuminated in **Figure 4**, #6. On this day, the southern polar fields had recently peaked in positive magnetism. We compare that event to the other largest events of the last few years:
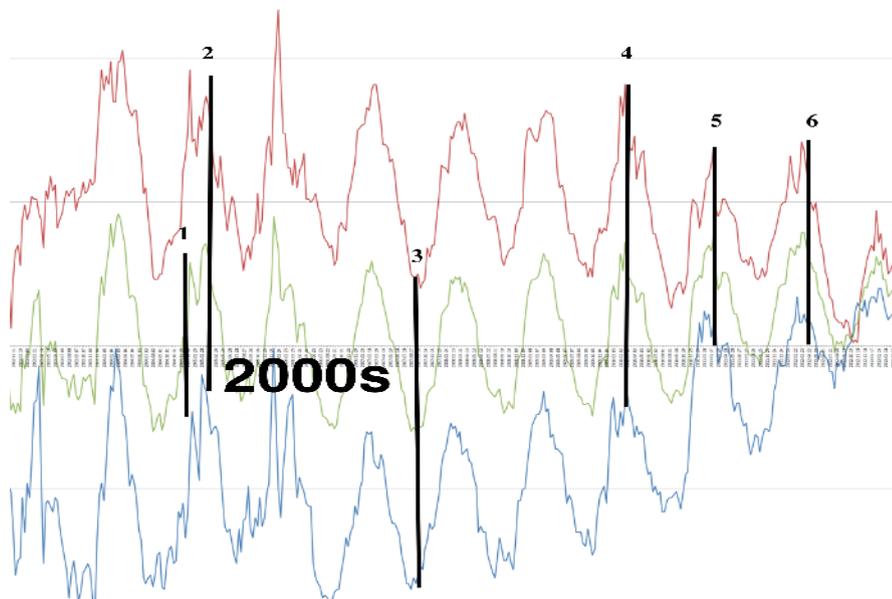

Fig. 4. The Six Largest Earthquakes of the Current Solar Polar Fields Cycle. A close-up of the Polar Maximum of the 2000s/2010s with black vertical lines at the 6 largest earthquakes of this the period. 5 of the 6 fell within 'Significant Windows'. (1) M9.1 Sumatra. December 26, 2004. Occurred during an "Average Reversal." (2) M8.6 Sumatra. March 28, 2005. Occurred during a positive peak of the southern field. (3) M8.5 Sumatra. September 12, 2007. Occurred during a negative peak of the northern field/positive trough of the southern field. (4) M8.8 Chile. February 27, 2010. Occurred during a positive peak of the southern field/negative trough of the northern field. (5) M9.0 Japan.

March 11, 2011. Occurred during a positive peak of the southern field. (6) M8.6 Sumatra. April 11, 2012. Occurred just after a positive peak of the southern field. In this figure the Average Fields curve is green.

In **Figure 4** we see #1 takes place during the Significant Window of an Average Reversal, #s 2, 4 and 5 all falling in Significant Windows of the positive peaks in southern field magnetism, #3 falls within the Significant Window around a negative peak in northern field magnetism, and only #6 fails to fall within a Significant Window. However, if you see how it closely follows the positive peak in southern fields, as did the previous two massive earthquakes, one must speculate if #6 failed to be 'covered by the Significant Windows' only because we failed to adequately understand the SPF effects. In fact, #6 looks like it *should* be covered by that peak, but it happened a few days too late according to our algorithm. Is that our error or an unrelated event? #6 actually represents two M8+ earthquakes that struck that day, so missing #6 means missing two M8+ earthquakes.

Refinement of the algorithm to add a few more significant days would pale in comparison to adding 3 or 4 of the M8 events to the list of those 'covered by the Significant Windows'. If we could cover 45% of the days under significant windows and 85-90% of the earthquakes it would certainly be worth a more complex approach than the first step identified here.

There were No M8+ Events during Polar Recovery
We also note that there were no M8+ earthquakes during Polar Recovery, and this was not a consideration in the algorithm. This lack of large earthquakes during Polar Recovery makes perfect sense if there is a relationship between solar activity and earthquakes as the data strongly suggests; there are neither pole reversals nor strong magnetism during those times, and the Significant Windows are currently focused on those factors. The final model provides historical coverage of 41.64% of days between July 5, 1976, and January 17, 2014. However, this coverage is not uniform across the phases of the solar polar cycle. In Polar Maximum, 46.54% of the days are covered, but in Polar Minimum and Recovery, 27.89% and 25.21% of the days are covered, respectively. Simply by eliminating the period of Polar Recovery the number total days in Significant Windows would decrease a few percentage points without 'covering' any fewer M8+ earthquakes.

Modeling the SPF earthquake trigger
To explain the connection between earthquakes and the changes in SPF, we consider modeling the Earth as a capacitor (Hill, 1971; Gregori, 2002; Ustundag, 2005) which could temporarily store energy to be triggered later by changes in the SPF. The SPF may also dictate how the electromagnetic characteristics of the solar wind help charge or discharge the earth. The ionosphere, an electrically conductive layer, could be treated as one plate of the capacitor while the other conducting plates exist in or below the ground. Two plates are separated by the Earth's atmosphere and mantle crust, which are treated as leaky insulations. In this model, electrical movements in the ionosphere in longitude (compression/expansion) or tangential (circulation) directions can result in significant changes in Earth's electric fields or magnetic fields which propagate into the Earth's crust, as part of the capacitor.

The field modulation (especially in the electric fields) influences the movement of global charges currently existing in the Earth's crust (Namgaladze, 2013), accelerating charge diffusion toward the tectonic hot spots that already contain high charge concentration. It is also known that charges are scattered in the uniform dielectric volume and converged around cracks or contacts between two dielectric layers containing stress. As a result, a strong electric field may be locally produced amplifying the mechanical stress through piezoelectric effect (Manbachi, 2011). Large displacement current and local heating have been observed during earthquakes as a result of electrical discharge in various earthquake preparation zones (Teisseyre, 1997; Lovett, 2013).

How might the SPF interact with Earth?
The Earth orbits the Sun in an electric field of charged solar wind known as the heliospheric current sheet or interplanetary current sheet. Space weather events such as sector boundary crossings are partially dependent on the polar fields (Svalgaard, 1974), which can stream away from the Sun near the north and south boundaries of the current sheet itself (**Figure 5**). The Earth may be directly interacting with these fields, or nearby currents and fields induced by the SPF, as the changes in earth's heliospheric latitude take

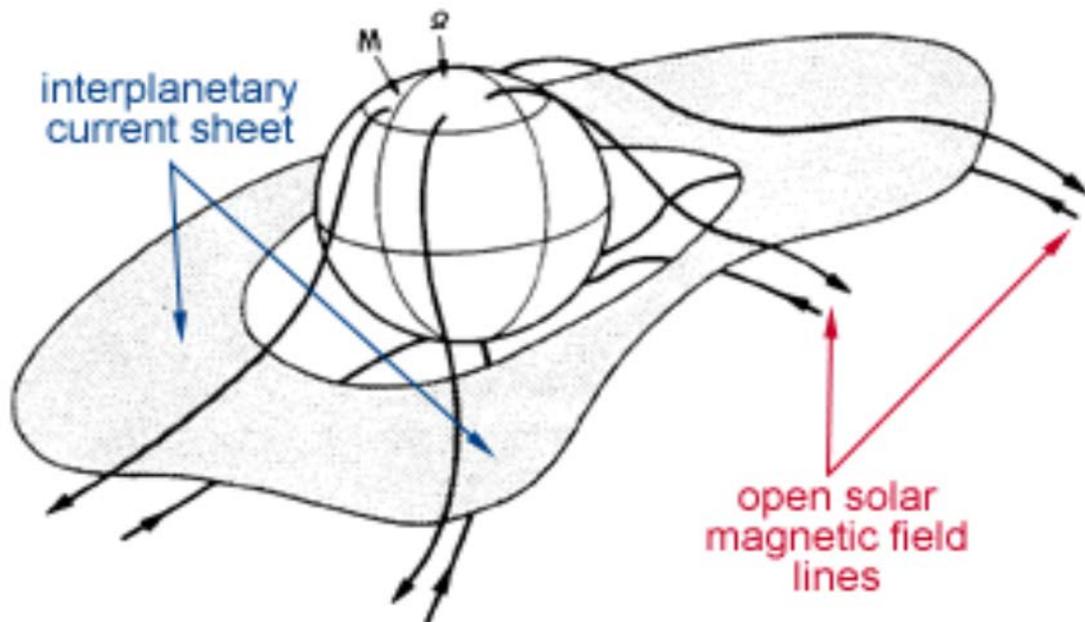our planet up and down through the current sheet.

Fig. 5. Lowest-Latitude Polar Fields Interact With Solar Wind. The lowest-latitude polar fields are interacting with the current sheet, and the Earth's orbit takes it through the north/south expanse of the sheet. "The cartoon showing the tilted current sheet and open solar magnetic field lines is adapted from Smith et al., Observations of the interplanetary sector structure up to heliographic latitudes of 16 degrees: Pioneer 11, *J. Geophys. Res*., v. 83, no. 717, 1978. The artist's conception of the heliospheric current sheet was obtained from J. Todd Hoeksema, Stanford University." xuv.byu.edu/docs/previous_research/euv_imager/documentation/part3/3IMF.html.

Studies confirm that the SPF also influences the solar wind; the solar wind is primary in the solar-terrestrial interaction and its modulation is dependent on space weather parameters at the star itself and in the interplanetary magnetic field, both of which are also highly dependent on the SPF (Svalgaard, 1978; Wang, 2009). The fluctuation in magnetic fields observable at the Sun is directly related to the fluctuation of space weather surrounding the Earth, often having direct integration into Earth's systems through magnetic portals (Phillips, 2008). The SPF reversal and the poleward migration of the neutral magnetic line described by Makarov et al. (1982) have significant effects on sunspot position and solar/geomagnetic indices. The same study found that solar prominences are tied to the movement of the SPF. The strength of the polar fields also modulate the appearance of equatorial coronal holes (Gibson, 2009). These are all potential pieces to the larger puzzle of how the SPF might interact with Earth to trigger the release of underground stress.

Electromagnetism and Earthquakes.
The SPF are solar-system-scale magnetic fields generated by the Sun, so electromagnetic exchanges are a worthwhile avenue of investigation for a mechanism explaining how the SPF trigger earthquakes. This is especially true since there is precedent for looking into the electromagnetic aspect of earthquakes. Scientists have documented magnetic field fluctuations before and during seismic events (Johnston, 1994; Scoville, 2014). "Earthquake lights" and strange clouds preceding earthquakes have spurred investigations into atmospheric and ionospheric precursors to those events (Pulinets, 2004; Namgaladze, 2009; Freund, 2009). Significant variations in energetic indices like the total electron content (TEC) or critical frequency of the ionosphere, preceded the great earthquakes of China/Haiti in 2008/2010 (Zolotov, 2010), Chile in 2010 (Yao, 2012) and Japan in 2011 (Kamogama, 2013). There is *extensive* research that describes potential coupling mechanisms between the ionosphere, the atmosphere and the ground, where electromagnetic interactions play an important role in the earthquake triggering process (Sorokin, 2005; Sorokin, 2006; Rycroft, 2006; Pulinets, 2011; Pulinets, 2014). The Sun may play a significant role in total electron content variations and other ionospheric-atmospheric interactions. (Mende, 2004; Liu, 2009).

At a meeting of the American Geophysical Union in December 2012, Tom Bleier described the electric currents associated with large earthquakes as "lightning underground," often exceeding 1 million amperes, and he states that static electricity is the key to predicting earthquakes (Lovett, 2013). Some have pegged the trigger for these currents, and the resulting seismic and volcanic events, to be solar activity (Odintsov 2007; Khain 2007/2008; U-yen 2014). Studies have shown that penetration of the L = 2.0 force line into seismic areas can be proliferative of earthquake activity, and the genesis of the earthquakes themselves may be electric currents flowing into the global electric circuit (Zhantayev, 2014; Khachikyan, 2014).

The Coming Solar Cycle(s)
The multi-decade decrease in SPF strength seen in **Fig. 1** is continuing now during a well-recognized weak solar cycle which some have speculated may soon mirror a grand minimum period like the Maunder or Dalton sunspot minima (Casey, 2014). The latest SPF Polar Reversal lasted twice as long as any other on record, and future cycle segments may not so-easily fit into categories or offer such easily discernable patterns. A change in SPF patterns may hint at further model refinements that will need to be made. The authors are particularly interested in any possible relationship between large earthquakes in Polar Maximum (sunspot minimum) and the large earthquakes expected to occur during a solar hibernation (grand sunspot minimum) phase (Choi and Tsunoda, 2011), because both involve periods of time that are traditionally considered to be calm and quiet on the Sun.

Scope of the Relationship
It is difficult to model this relationship in a lab, but if we are looking into the charge/discharge phases of a capacitor model then we must eventually ask where this charging originates. We can assume that the Sun is a primary source under that model, but extrasolar sources of Earth's and Sun's charging should also be considered.

The well-known "wind-up problem," which sees galaxy arms maintaining form over time instead of thinning to extinction, demonstrates that gravity is not the lone force controlling the actions of the Milky Way. If there are interstellar magnetic fields with other stars or the galactic center (like IMF in the solar system), then the genesis of these energetic interactions may be defined on scales beyond the heliosphere.

CONCLUSION
The solar polar fields are known to influence space weather and the near-Earth space environment. This analysis is indicative of a significant relationship between the SPF and Earth's largest seismic events. The extremes in magnetism and reversals in polarity represent the times of significant heliospheric magnetism on a local scale, and there is ample evidence to suggest that electromagnetic triggers of tectonic stress are a worthwhile mechanism to consider. After Gregori (2002) it stands to reason that any piece of the puzzle connecting Earth and Sun (and milkyway) is worthy of further investigation, and the SPF certainly fit the criteria.

References Cited
Babcock, H.W. and Babcock, H.D., 1955. The Sun's Magnetic Field, 1952-1954. *Ap. Jour.*, v. 121, p. 349.
Babcock, H.D., 1959. The Sun's Polar Magnetic Field. *Ap. Jour.,* v. 130, p. 364.
Choi, D. R. and Tsunoda, F., 2011. Volcanic and seismic activities during the solar hibernation periods. *New Concepts in Global Tectonics Newsletter*, no. 61, p. 78-87.
Freund, F.T., Kulachi, I.G., Cyr, G., Ling, J., Winnick, M., Tregloan-Reed, J. and Freund, M. M,, 2009. Air Ionization at Rock

Surfaces and Pre-Earthquake Signals. *Jour. Atmo. Sol.-Terr. Phys.,* v. 71, nos. 17-18, p. 1824-1834.

Gibson, S. E., Kozyra, J. U., Toma, G., Emery, B. A., Onsager, T. and Thompson, B.J., 2009. If the Sun is so quiet, why is the Earth ringing? A comparison of two solar minimum intervals. *Jour. Geophys. Res.,* v. 114(A9), p. 105.

Gregori, G.P., 2002. Galaxy-Sun-Earth Relations. *Beitrage zur Geschichte der Geophysik und Kosmischen Physik,* Band 3, Heft 4.

Hill, R. D., 1971. Spherical capacitor hypothesis of the earth's electric field. Jour. *Pure and Applied Geophysics,* v. 84, no. 1, p. 67-74.

Holloman, C., 2014. Appendix C: Solar Polarity Algorithm. [Published in advance for open review] http://www.suspicious0bservers.org/wp-content/uploads/2014/09/Appendix-C.pdf

Johnston, M.J.S., Mueller, R.J. and Sasai, Y., 1994. Magnetic field observations in the near-field the 28 June 1992 M7.3 Landers, California earthquake. *Bull. Seis. Soc. Am.,* v. 84, p. 792-798.

Kamogawa, M. and Kakinami, Y., 2013. Is an ionospheric electron enhancement preceding the 2011 Tohoku-Oki earthquake a precursor? *Jour. Geophys Res Space Physics,* v. 118, p. 1-4.

Khachikyan, G., Inchin, A. and Toyshiev, N., 2014. Solar modulation of earthquake occurrence in areas penetrated by L of 2.0 populated by anomalous cosmic rays. *40th COSPAR Scientific Assembly:* Abstract C4.1-49-14.

Khain, V.E. and Kalilov, E.N., 2007/2008. About the possible influence of solar activity upon seismic and volcanic activities: long-term forecast. *Science Without Borders* - Transactions of the International Academy of Science, H&E 3, p. 316-334.

Lovett, R., 2013. Scientists Seek Foolproof Signal to Detect Earthquakes. *National Geographic News.* http://news.nationalgeographic.com/news/2013/01/04-earthquakees-defy-prediction-efforts/

Liu, L. and Chen, Y., 2009. Statistical analysis of solar activity variations of total electron content derived at Jet Propulsion Laboratory from GPS observations. *Jour. Geophys. Res.,* v. 114(A10), p. 311.

Makarov, V. and Fatianov, M., 1982. Poleward Migration of the Magnetic Neutral Line and the Reversal of the Polar Fields on the Sun. *Sol. Phys.,* v. 85, no. 2, p. 215-226.

Manbachi, A. and Cobbold, R.S., 2011. Development and application of piezoelectric materials for ultrasound generation and detection. *Ultrasound,* v. 19, no. 4, p. 187-196.

Mende, S., 2004. Monitoring geospace responses to solar variability by global imaging. *Living With a Star Workshop* - Session 3: Oral Powerpoint Presentation. http://lasp.colorado.edu/sdo/meetings/session_1_2_3/presentations/session3/3_10_Mende.pdf

Namgaladze, A.A., 2013. Earthquakes and Global Electrical Circuit. *Russ. Jour. Physical Chemistry,* v. B 7, no. 5, p. 589-593.

Namgaladze, A.A., Zolotov, O.V., Zakharenkova, I.E., Shagimuratov, I.I. and Martynenko, O.V., 2009. Ionospheric total electron content variations observed before earthquakes: Possible physical mechanism and modeling. *Proc. MSTU*, v. 12, no. 2, p. 308-315.

Odintsov, S.D., Ivanov-Kholodnyi,G. S. and Georgieva, K., 2007. Solar activity and global seismicity of the earth. *Bull. Russ. Aca. Sci. Phys.,* v. 71, no. 4, p. 593-595.

Phillips, T., 2008. Magnetic Portals Connect Earth to the Sun. *NASA Sci.* http://science.nasa.gov/science-news/science-at-nasa/2008/30oct_ftes/

Pulinets, S., 2014. Electromagnetic Effects in the Atmosphere, Ionosphere and Magnetosphere Initiated by the Earthquake Preparation Process. General Assembly and Scientific Symposium (URSI GASS) Conference August 2014.

Pulinets, S., and Boyarchuk, K., 2004. Ionospheric Precursors of earthquakes. *Springer*, ISBN 3-540-20839-9.

Pulinets, S. and Ouzounov, D., 2011. Lithosphere-Atmosphere-Ionosphere Coupling (LAIC) model - An unified concept for earthquake precursors validation. *Jour. Asian Earth Sci.,* v. 41, nos. 4-5, p. 371-382.

Scoville, J., Heraud, J. and Freund, F.T., 2014. Pre-earthquake Magnetic Pulses. arXiv Cornell University Library. arXiv:1405.44821.

Rycroft, M.J., 2006. Electrical processes coupling the atmosphere and ionosphere: An overview. *Jour. Atmos, Sol,-Terr, Phys,* v. 68, nos. 3-5, p. 445-456.

Sorokin, V.M., Yaschenko, A.K. and Hayakawa, M., 2006. Formation Mechanism of the Lower-Ionosphere Disturbances by the Atmospheric Electric Current over a Seismic Region. *Jour. Atmos. Sol.-Terr. Phys.*, v. 8, no. 11, p. 1260-1268.

Sorokin, V.M., Yaschenko, A.K., Chmyrev, V. M., Hayakawa, M., 2005. DC electric field amplification in the mid-latitude ionosphere over seismically active faults. *Nat Hazards Earth Syst, Sci., v.* 5, p. 661-666.

Svalgaard, L, Wilcox, J.M. and Duvall, T.L., 1974. A model combining the polar and the sector structured solar magnetic fields. *Sol. Phys.,* v. 37, no. 1, p. 157-172.

Svalgaard, L., Duval, T. and Scherrer, P., 1978. The Strength of the Sun's Polar Fields, *Sol. Phys.,* v. 58, p. 225-240.

Teisseyre, R., 1997. Generation of electric field in an earthquake preparation zone. *Annals of Geophys.,* v. 40, no. 2, p. 297-304.

Ustundag, B., Kalenderli, O. and Eyidogan, H., 2005. Multilayer Capacitor Model of the Earth's Upper Crust. *Turk Jour. Elec. Engin.*, v.13, no.1, p. 163-173.

U-Yen, K., 2014. Evidences of Space Weather Induced Natural Disasters. Electric Universe Conference 2014 in Albuquerque, NM.

Wang ,Y.M., Robbrecht, E. and Sheeley, Jr. N.R., 2009. On the Weakening of the Polar Magnetic Fields During Solar Cycle 23. *Ap. Jour.,* v. 707, no. 2, p. 1372-1386.

Yao, Y.B., Chen, P., Zhang, S., Chen, J.J., Yan, F. and Peng, W.F., 2012. Analysis of pre-earthquake ionospheric anomalies

before the global M = 7.0+ earthquakes in 2010. *Nat Hazards Earth Syst. Sci.,* v. 12, p. 575-585.

Zhantayev, Z., Khachikyan, G. and Breusov, N., 2014. On dependence of seismic activity on 11 year variations in solar activity and/or cosmic rays. EGU General Assembly: Abstract id.5253.

Zolotov, O., Prokhorov, B., Namgaladze, A. and Martyneko, O., 2010. TEC anomalies before the Haiti Jan. 12, 2010 and China May 12, 2008 earthquakes. *38th COSPAR Scientific Assembly*: 5.

Appendix A

The following is a description of the mathematical model used to identify periods of increased likelihood of large earthquakes (*i.e.*, earthquake windows). We begin by defining some of the notation used throughout the description. We use t as an index of days, starting with 1976-06-04 as $t = 1$. Let $t \in \{1, 2, ..., T\}$, where $T = 13741$, corresponding to 2014-01-17. Since solar polarity observations are only available every 10 days, we create a second time index, r, where $r = 1 + (\frac{t-1}{10})$ when $mod(t, 10) = 1$ and is undefined otherwise, so $r \in \{1, 2, ..., R\}$, where $R = 1375$. We use N_r to denote the magnitude of the north pole on day r and S_r to denote the magnitude of the south pole on day r in μT.

Identifying Solar Maximum, Minimum, and Recovery

For each r, we first determine whether the sun is in a period of solar maximum, minimum, or recovery. Identifying these phases requires identification of the peaks and troughs of both the long-term cycles and minicycles of each of the poles. To identify peaks and troughs of the long-term cycles, we take a rolling average of the magnitude and identify the maximal (and minimal) points within 2000-day rolling windows. We define

$$A_{N,r} = \frac{\sum_{i=r-100}^{r+99} N_i}{200},$$

the rolling average of the north pole at time r,

$$M_N^1 = \left\{ r : A_{N,r} = max_{i=r-100}^{r+99}\{A_{N,i}\} \right\},$$

the set of long-term local maxima for the north pole, and

$$M_N^2 = \left\{ r : A_{N,r} = min_{i=r-100}^{r+99}\{A_{N,i}\} \right\},$$

the set of long-term local minima for the north pole. Long-term extremes of the south pole are defined similarly. For simplicity of notation throughout this manuscript, we have ignored the fact that indexes exceed the limits of the data ($r < 1$ or $r > R$). In the actual implementation, indexes and values that depend on them (like the denominator of A) are adjusted according to the number of available observations in a 2000-day window.

To identify mini-cycles, we fit local sine wave functions (trended, phase shifted, and scaled) with a period of 1 year at each time point and average across fitted values of several locally fitted functions. For the north pole, for each r we fit the following statistical model:

$$N_i \sim No\left(\beta_{0Nr} + \beta_{1Nr}i + \beta_{2Nr}\sin\left(\frac{2\pi10i}{365}\right) + \beta_{3Nr}\cos\left(\frac{2\pi10i}{365}\right), \sigma_{Nr}^2\right),$$

for $i \in \{r - 100, r - 99, ..., r + 99\}$, where $No(\cdot, \cdot)$ represents the normal distribution with specified mean and variance. Defining $\widehat{N_{rr'}}$ as the fitted value of N_r for the model at r', the smoothed mini-cycle is defined as

$$U_{Nr} = \sum_{i=r-99}^{r+100} \widehat{N_{ri}} / 200.$$

The local maxima and minima of the mini-cycles are then defined as the local maxima and minima of U_{Nr} (*i.e.*, values of r for which the two adjacent points have greater (or lower, in the case of minima) magnitude).

For $r = 1$, the sun is, by definition, in the polar maximum phase. The time points $r = 2, 3, \ldots, R$ are assessed sequentially with the phase being the same as the preceding point unless a transitional event happens. The transition from polar maximum to polar minimum occurs at the first time that the second of the two poles exhibits a reversal across the equator. Mathematically, if the current phase of polar maximum is one in which the north pole reached a maximum and the south pole reached a minimum, the transition to polar minimum occurs at $\max\{\min\{r': N_{r'} < 0\}, \min\{r': S_{r'} > 0\}\}$, where r' is later than the start of the polar maximum. The transition from polar minimum to polar recovery occurs at the last time that either of the poles exhibits a force directionally the same as its most recent maximum or minimum (and before the next long-term maximum or minimum). Again, if the most recent phase of polar maximum was one in which the north pole reached a maximum and the south pole reached a minimum, the transition to polar recovery occurs at $\max\{\max\{r': N_{r'} > 0\}, \max\{r': S_{r'} < 0\}\}$, where r' is later than the start of the polar minimum and earlier than the next long-term maximum or minimum. The transition from polar recovery to polar maximum always occurs 1.5 years after the transition to polar recovery.

Identifying Spikes

The values of U_{Nr} and U_{Sr} represent smoothed versions of the solar cycles that preserve both long-term trends and the approximately 1-year minicycles of the poles. The next step of the algorithm uses those smoothed representations to divide the modeled time span into segments representing half-minicycles. This segmenting is performed separately for each of the poles, and, for simplicity, we only describe the method for the north pole. For each adjacent pair of local maxima and minima in U_{Nr}, we identify a segmenting time point r where the value of N_r is as close as possible to the average of the polar force at the maximum and minimum. Mathematically, if r' and r'' represent a pair of time points for which U_{Nr} is at adjacent maximums and minimums, the segmenting time point is $argmin_r|N_r - \frac{1}{2}(N_{r'} + N_{r''})|$.

These segmenting points divide the span into half-minicycles, and each half-minicycle is classified as convex or concave, depending on whether the local maximum within the half-minicycle is a maximum or minimum. To simplify further notation, we introduce a new pair of indexes, q_N and q_S, indexing half-minicycles in the north and south poles, respectively. For the time period in this study, there are 79 half-minicycles of the north pole and 75 half-minicycles of the south pole, so $q_N \in \{1, 2, \ldots, 79\}$ and $q_S \in \{1, 2, \ldots, 75\}$.

Within each half-minicycle, we identify spikes using a series of rules. For simplicity, these rules are described for concave half-minicycles (in the north pole); applying them to convex half-minicycles is just a matter of reversing the sign of the magnitudes of the poles. Within a half-minicycle q_N, define the set of time points in q_N as

$Q_{q_N} = \{r : r \geq \text{ the segmenting point beginning } q_N \text{ and } r \leq \text{ the segmenting point ending } q_N\}$.

We first identify the time points of the maximal polar force within the half-minicycle $P_{q_N} = \{r : r \in Q_{q_N} \text{ and } r \geq N_{r'} \; \forall \; r' \in Q_{q_N}\}$ and identify these points as spikes. Starting with the minimal value in P_{q_N}, we sequentially examine each smaller value in the set Q_{q_N} and assess two conditions:

1. Is the polar force at the examined time point more than 10 greater than the smallest polar force between the examined time point and the last identified spike?
2. Is the polar force of all remaining time points between the examined time point and the end of the set Q_{q_N} smaller than the polar force at the examined time point?

If both of these conditions are satisfied, the examined time point is identified as an additional spike within the half-minicycle and we proceed to evaluate the next smaller value in the set Q_{q_N}. Once these criteria have been applied to all time points from the smallest value in P_{q_N} to the smallest value in Q_{q_N}, the process is repeated starting with the maximal value in P_{q_N} and sequentially examining each larger value in the set Q_{q_N}.

At the end of applying the above procedure, each half-minicycle has, identified within it, one or more time points at which the polar force is spiking. We use P'_{q_N} to denote the full set of spike times within the half-minicycle q_N. Note that $P_{q_N} \subseteq P'_{q_N}$. For each r in P'_{q_N}, the spike is classified as primary or secondary and as being peaked, semi-flat, or completely flat. A spike is classified as secondary if the polar force at the time of the spike is at least 10 μT less than the magnitude of the maximal force exhibited in q_N. To determine whether a spike is peaked, semi-flat, or completely flat, we examine the polar force for all adjacent time points with a polar force no more than 10 μT less than the polar force at the spike. If at least one of the adjacent time points has a force no more than 3 μT less than the polar force at the spike, it is classified as semi-flat. If any of the adjacent time points has a force exactly equal to the spike, it is classified as completely flat.

After identifying all of the spikes and classifying them as primary/secondary and peaked/semi-flat/completely flat, we define each half-minicycle as being a single, double, triple, or quadruple period. This classification is made based solely on the number of primary spikes in the half-minicycle.

Identifying Earthquake Windows

Define a function $f(r) = 1 + 10(r - 1)$ that converts the r index of 10-day periods to a corresponding day index in $\{1, 2, ..., T\}$. Also, define the average polarity at time r as $B_r = (N_r + S_r)/2$. Then, a day t is in an earthquake window if any of the following conditions are met:

1. There exists a spike at some time r' in some set P'_{q_N} such that (a) r' is in a period of solar maximum, (b) the half-minicycle q_N is a single or double period, (c) the spike at time r' is peaked and primary, (d) $N_{r'}$ has the same sign as $N_{min(Q_{q_n})}$ and $N_{max(Q_{q_n})}$, (e) $\left|N_{\min(P_{q_n})} - N_{\min(P_{q_n-1})}\right| \geq 40\mu$T, (f) $\left|N_{\min(P_{q_n})} - N_{\min(P_{q_n+1})}\right| \geq 40\mu$T, and (g) $|f(r') - t| \leq 20$.

2. There exists a spike at some time r' in some set P'_{q_N} such that (a) r' is in a period of solar maximum, (b) $|N_{r'}| > 175\mu$T, (c) the half-minicycle q_N is a single period, (d) the spike at time r' is peaked and primary, (e) $N_{r'}$ has the same sign as $N_{min(Q_{q_n})}$ and $N_{max(Q_{q_n})}$, (f) $\left|N_{\min(P_{q_n})} - N_{\min(P_{q_n-1})}\right| \geq 40\mu$T, (g) $\left|N_{\min(P_{q_n})} - N_{\min(P_{q_n+1})}\right| \geq 40\mu$T, and (h) $|f(r') - t| \leq 25$.

3. There exists a spike at some time r' in some set P'_{q_N} such that (a) r' is in a period of solar maximum, (b) the half-minicycle $q_N - 1$ is a single period with some r'' such that $|N_{r''}| > 175\mu$T, (c) the half-minicycle $q_N + 1$ is a single period with some r''' such that $|N_{r'''}| > 175\mu$T, (d) the half-minicycle q_N is a single period, (e) $N_{r'}$ has the same sign as $N_{min(Q_{q_n})}$ and $N_{max(Q_{q_n})}$, (f) $\left|N_{\min(P_{q_n})} - N_{\min(P_{q_n-1})}\right| \geq 40\mu$T, (g) $\left|N_{\min(P_{q_n})} - N_{\min(P_{q_n+1})}\right| \geq 40\mu$T, and (h) $|f(r') - t| \leq 25$.

4. There exists a spike at some time r' in some set P'_{q_N} such that (a) r' is in a period of solar maximum, (b) $|S_{r''}| > 175\mu$T, where $r'' = \max\{r: r < r'$ and $r \in P'_{q_S}$ for some $q_S\}$, (c)

$|S_{r'''}| > 175\mu T$, where $r''' = \min\{r: r > r' \text{ and } r \in P'_{q_S} \text{ for some } q_S\}$, (d) the half-minicycle q_N is a single period, (e) $N_{r'}$ has the same sign as $N_{min(Q_{q_n})}$ and $N_{max(Q_{q_n})}$, (f) $\left|N_{min(P_{q_n})} - N_{min(P_{q_{n-1}})}\right| \geq 40\mu T$, (g) $\left|N_{min(P_{q_n})} - N_{min(P_{q_{n+1}})}\right| \geq 40\mu T$, and (h) $|f(r') - t| \leq 25$.

5. There exists a spike at some time r' in some set P'_{q_N} such that (a) r' is in a period of solar maximum, (b) the half-minicycle q_N is a triple period, (c) the spike at time r' is peaked and primary, (d) $N_{r'}$ has the same sign as $N_{min(Q_{q_n})}$ and $N_{max(Q_{q_n})}$, (e) $\left|N_{min(P_{q_n})} - N_{min(P_{q_{n-1}})}\right| \geq 40\mu T$, (f) $\left|N_{min(P_{q_n})} - N_{min(P_{q_{n+1}})}\right| \geq 40\mu T$, and (g) $|f(r') - t| \leq 15$.

6. There exists a spike at some time r' in some set P'_{q_N} such that (a) r' is in a period of solar maximum, (b) the half-minicycle q_N is a quadruple period, (c) the spike at time r' is peaked and primary, (d) $N_{r'}$ has the same sign as $N_{min(Q_{q_n})}$ and $N_{max(Q_{q_n})}$, (e) $\left|N_{min(P_{q_n})} - N_{min(P_{q_{n-1}})}\right| \geq 40\mu T$, (f) $\left|N_{min(P_{q_n})} - N_{min(P_{q_{n+1}})}\right| \geq 40\mu T$, and (g) $|f(r') - t| \leq 10$.

7. There exists a spike at some time r' in some set P'_{q_N} such that (a) r' is semi-flat, (b) $N_{r'}$ has the same sign as $N_{min(Q_{q_n})}$ and $N_{max(Q_{q_n})}$, (c) $\left|N_{min(P_{q_n})} - N_{min(P_{q_{n-1}})}\right| \geq 40\mu T$, (d) $\left|N_{min(P_{q_n})} - N_{min(P_{q_{n+1}})}\right| \geq 40\mu T$, and (e) $|f(r') - t| \leq 10$.

8. There exists a spike at some time r' in some set P'_{q_N} such that (a) r' is completely flat, (b) $N_{r'}$ has the same sign as $N_{min(Q_{q_n})}$ and $N_{max(Q_{q_n})}$, (c) $\left|N_{min(P_{q_n})} - N_{min(P_{q_{n-1}})}\right| \geq 40\mu T$, (d) $\left|N_{min(P_{q_n})} - N_{min(P_{q_{n+1}})}\right| \geq 40\mu T$, and (e) $|f(r') - t| \leq 15$.

9. There exists a spike at some time r' in some set P'_{q_N} such that (a) r' is secondary, (b) $N_{r'}$ has the same sign as $N_{min(Q_{q_n})}$ and $N_{max(Q_{q_n})}$, (c) $\left|N_{min(P_{q_n})} - N_{min(P_{q_{n-1}})}\right| \geq 40\mu T$, (d) $\left|N_{min(P_{q_n})} - N_{min(P_{q_{n+1}})}\right| \geq 40\mu T$, and (e) $|f(r') - t| \leq 10$.

10. There exists some time r' such that (a) $sign(N_{r'}) = -sign(N_{r'-1})$, (b) there exists some $r'' \in [\max\{r: r < r' \text{ and } sign(N_r) = -sign(N_{r-1})\}, r' - 1]$ such that $|N_{r''}| > 15\mu T$, (c) there exists some $r''' \in [r' + 1, \min\{r: r > r' \text{ and } sign(N_r) = -sign(N_{r+1})\}]$ such that $|N_{r'''}| > 15\mu T$, and (d) $|f(r') - t| \leq 15$.

11. There exists some time r' such that (a) $r' - 1$ is during solar maximum, (b) $sign(N_{r'}) = -sign(N_{r'-1})$, (c) there is no $r'' < r'$ in the same period of solar maximum as $r' - 1$ for which $sign(N_{r''}) = -sign(N_{r''-1})$, and (d) $|f(r') - t| \leq 15$.

12. There exists some time r' such that (a) solar minimum ends at r' and (b) $|f(r') - t| \leq 15$.

13. There exists some time r' such that (a) $sign(B_{r'}) = -sign(B_{r'-1})$, (b) either the phase is solar maximum at time r' or the following two conditions are satisfied
    a. there exists some $r'' \in [\max\{r: r < r' \text{ and } sign(B_r) = -sign(B_{r-1})\}, r' - 1]$ such that $|B_{r''}| > 50\mu T$
    b. there exists some $r''' \in [r' + 1, \min\{r: r > r' \text{ and } sign(B_r) = -sign(B_{r+1})\}]$ such that $|B_{r'''}| > 50\mu T$,
    (c) $\min\{r: r > r' \text{ and } sign(B_r) = -sign(B_{r+1})\} - r' \leq 9$, and (d) $|f(r') - t| \leq 15$.

For conditions $1 - 11$, identical conditions using the south pole also apply.

The above conditions determine whether each time point falls into an earthquake window, but the occurrence of earthquakes can reduce the likelihood of a subsequent earthquake, requiring shifting of windows that occur soon after. Each time a large earthquake (8+ magnitude) or series of slightly smaller earthquakes (4 7.5+ magnitude quakes in a 100 day window) occurs, earthquake windows occurring in the next 100 days are delayed. For earthquake windows starting less than 30 days after the occurrence of one of these earthquake events, the window is pushed back by the minimum of either 20 days or half the width of the interval for the condition above that created the earthquake window. For earthquake windows starting between 31 and 100 days after the occurrence of one of these earthquake events, the window is pushed back by 10 days.